Supporting information

Phosphorus adsorption on blast furnace slag with different magnetism and its potential for phosphorus recovery

Xiaoxin Wu[1], Rui Zhan[2], Lili Liu [2,*], Jinjing Lan[3], Ning Zhao[1], Zhiping Wang [1,3,*]

[1] China-UK low Carbon college, Shanghai Jiao Tong University, Shanghai 200240, China; wu-xiaoxin@sjtu.edu.cn (X.W.); 17866624931@163.com (N.Z.)
[2] State Environmental Protection Key Laboratory of Environmental Risk Assessment and Control on Chemical Process, East China University of Science and Technology, Shanghai 200237, China; 18321687229@163.com (R.Z.)
[3] School of Environmental Science and Engineering, Shanghai Jiao Tong University, Shanghai 200240, China; arana-lan@sjtu.edu.cn (J.L.)
* Correspondence: wangzply@sjtu.edu.cn (Z.W.); lilyliu@ecust.edu.cn (L.L.)

Total page: 9

Tables :

Table S1. XRF determination revealed the Surface chemical composites of BFS with size of 1.0-2.0 mm.

Table S2. Binding energy and atomic composition of P in surface of BFS.

Table S3. Results of the Thomas model at different influent P concentration.

Table S4. Results of the Thomas model at different influent pH.

Table S5. Results of the Thomas model at different HRT.

Figures：

Figure S1. SEM-EDS detection of non-magnetic BFS1 after phosphorus adsorption.

Figure S2. The fluorescent components of urban sewage identified with PARAFAC analysis.

Table S1. XRF determination revealed the Surface chemical composites of BFS with size of 1.0-2.0 mm (Atomic percentage).

	Fe %	Mn %	Al %	Si %	K %
a	22.34	41.42	11.62	20.67	2.12
b	24.79	27.53	12.86	30.29	2.95
c	25.46	43.46	15.21	12.67	1.35
d	9.78	6.72	15.05	65.31	1.70
e	10.36	13.48	18.80	52.42	2.36
f	9.50	0.59	6.16	78.51	4.31

a.Magnetic BFS before adsorption; b. Magnetic BFS after adsorption; c. Magnetic BFS after leaching; c. Non-magnetic BFS before adsorption; d. Non-magnetic BFS after adsorption; e. Non-magnetic BFS after leaching.

Table S2. Binding energy and atomic composition of P in surface of BFS

Samples	B.E. (eV)		Atomic composition (%)	
	HPO_4^{2-}	$H_2PO_4^-$	HPO_4^{2-}	$H_2PO_4^-$
BFS-3	133.3	134.17	0.38	0.19
BFS-4	133.58	134.45	0.44	0.22
BFS-5	132.87	133.74	0.20	0.10
BFS-6	133.29	134.16	0.07	0.04

*BFS1 were separated as the magnetic samples (BFS-1, 3, 5) and non-magnetic samples (BFS-2, 4, 6), which were detected with the XPS as before P adsorption (BFS-1, 2) and after P adsorption (BFS-3, 4), as well as the regenerated samples (BFS-5, 6).

Table S3. Results of the Thomas model at different influent P concentration

C_0(mg L^{-1})	K_{Th} ($L \cdot mg^{-1} \cdot d^{-1}$)	q_0 (mg g^{-1})	R^2
5	0.5011	0.0726	0.9657
10	0.2509	0.1461	0.9773
20	0.1249	0.2848	0.9841

* The adsorption column was filled with 1675g BFS1, fed with C_0=5.0, 10.0 and 20 mg L^{-1} P solution and pH 7.0. The HRT was set as 2 hours, corresponded to filtration rate of 0.5m h^{-1}.

Table S4. Results of the Thomas model at different influent pH

pH	K_{Th} ($L \cdot mg^{-1} \cdot d^{-1}$)	q_0 ($mg\ g^{-1}$)	R^2
4	0.1986	0.1350	0.9969
7	0.2509	0.1461	0.9773
9	0.2609	0.1402	0.9854

* The adsorption column was filled with 1675g BFS1, fed with C0=10.0 mg L^{-1} P solution and pH of 4.0, 7.0 and 9.0. The HRT was set as 2 hours, corresponded to filtration rate of 0.5m h^{-1}.

Table S5. Results of the Thomas model at different HRT

HRT (h)	K_{Th} ($L \cdot mg^{-1} \cdot d^{-1}$)	q_0 ($mg\ g^{-1}$)	R^2
2	0.2325	0.1528	0.9707
4	0.1322	0.1412	0.9576

* The adsorption column was filled with 1675g BFS1, fed with C_0=10.0 mg L^{-1} P solution and pH 7.0. The filtration rate was set as 0.5 and 0.25 m h^{-1}, corresponded to HRT about 2 and 4 hours.

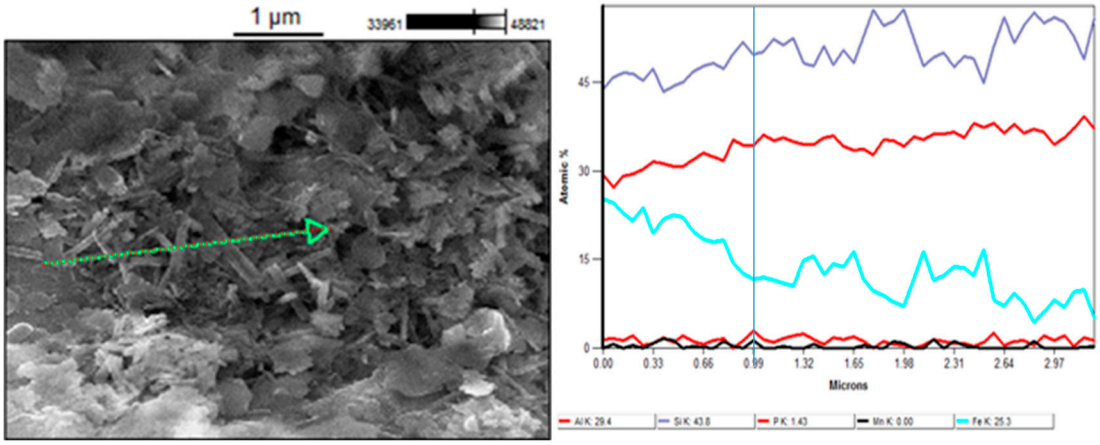

Figure S1. SEM-EDS detection of non-magnetic BFS1 after phosphorus adsorption.

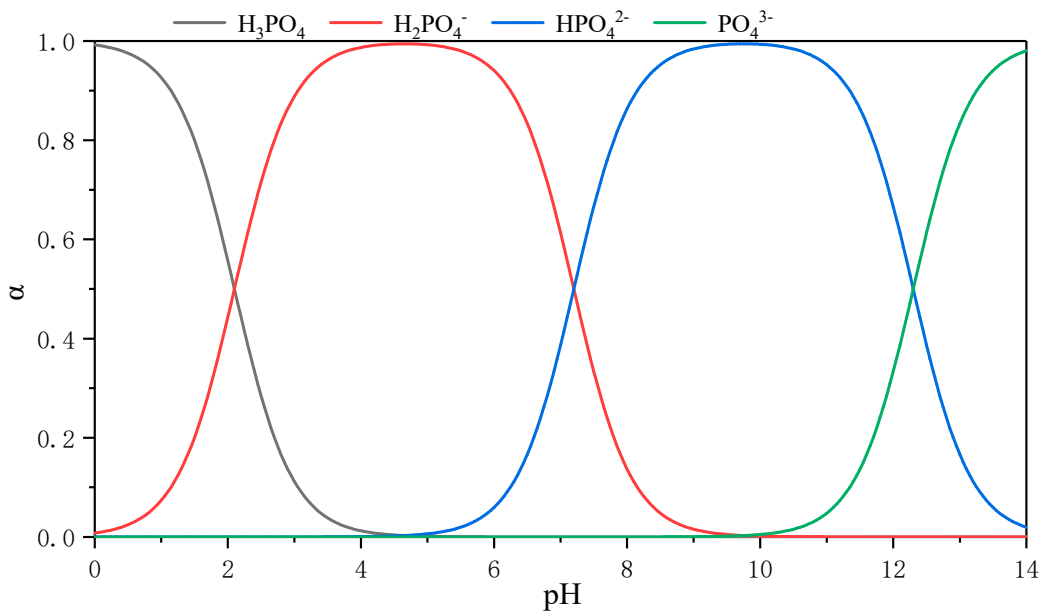

Figure S2. Species of orthophosphate varied with the pH